Modelling of the treatment of wastewater by photovoltaic solar electrochemical oxidation (PSEO) assisted by redox-flow batteries ~~for wastewater treatment.~~

*M. Millán, C.M. Fernández-Marchante, J. Lobato, P. Cañizares, M.A. Rodrigo**

Department of Chemical Engineering, Faculty of Chemical Sciences & Technologies, University of Castilla-La Mancha, Av. Camilo Jose Cela n 12, 13071 Ciudad Real, Spain

Abstract

This work aims at the formulation of simple and pragmatic models to predict the behaviour of a photovoltaic solar electrochemical oxidation treatment assisted by an energy storage system. Those models will be later integrated in a software tool that allows the optimization and the management of the energy provided by solar panels to power electrochemical advanced oxidation processes coupled with a redox flow battery as energy storage system. Models for a PV panel, a redox flow battery stack and a conductive diamond electrochemical oxidation electrolyzer have been proposed and fitted to experimental data. Results showed a huge accuracy of the models to predict the electric and remediation parameters. Validation analyses reported high regression coefficients above 0.96 which confirm the precision of all the proposed models. Thus, once known the solar radiation in a located place, the level of remediation of a wastewater effluent treated by electrolysis may be estimated. Furthermore, it must be pointed out that the operational conditions of the treatment could be optimized and adjusted by means of an energy storage in the redox flow battery. Considering those facts, the sustainability and efficiency of electrochemically-assisted remediation processes could be highly increased.

Keywords

Energy management; solar power; green sources; electrooxidation; redox flow batteries; forecasting; PV panels

Highlights

- Simple models reproduce satisfactory electric parameters with R^2 over 0.96.
- Reduction of organic pollutant concentration was fitted with R^2 over 0.99.
- Known the solar radiation, the generated solar power can be estimated.
- The solar power may distribute in order to be directly used or stored.

*Corresponding author. Telf: +34 926 295 300; fax: +34 926 295 256. E-mail address: manuel.rodrigo@uclm.es

1. Introduction

The awareness about global climate change has increased the concern of population and national governments which have engaged in efforts to achieve a sustainable development in the years to come. Nevertheless, the massive production and use of synthetic and harmful compounds in the last century have left many sites polluted by hazardous chemicals. Hence, the remediation of these natural locations is key to stop the spreading of pollutants and to prevent any additional adverse effects on the environment or the human health [1]. For this reason, its fast detection, containment, and removal from the contamination focus are essential actions to avoid an uncontrolled dispersion into the environment [2]. Until now, the research community has focused their studies on the search of more efficient remediation processes missing other essential criteria. Thus, to quantify the overall potential of developing remediation treatments, its economic, environmental and social impacts must be assessed simultaneously [3]. Economically, a remediation system must be designed as flexible as possible in order to be able to adapt them to treat new emerging pollutants [4], reducing in this way many of the cost related to these technologies. Regarding the environmental impact, it is of great importance to evaluate the sustainability of a remediation treatment to avoid additional pollution issues [5].

One of the most evaluated remediation technologies for the treatment of liquid wastes are the electrochemical advanced oxidation processes (EAOPs), which have exhibited huge efficiencies removing organic compounds from effluents [6-11]. Furthermore, these techniques have been reported as one of the cleaner and more sustainable remediation processes because they only need electricity for in-situ production of reagents. Studies reported that the sustainability of electrochemical processes is highly influenced by their

energy requirements [12] and claims in favor of using green energies to power those technologies [13]. Nevertheless, the renewable energies cannot provide a continuous and constant power supply, which may become a drawback when a treatment is operated at continuous mode. Previous studies showed that the direct coupling of renewable energies and EAOPs does not show a satisfactory removal of pollutant, although the negative effect was less prominent in other electrochemically-assisted technologies such as the soil electrokinetic treatments [14, 15]. At this point, it has been highlighted that the control of some operation conditions could trade off the negative impacts of lower solar radiation values during the direct powering of the electrochemical treatment [16-18]. Besides, despite the positive results reached working under this operational mode, smart control systems are required to ensure high levels of removal throughout the remediation treatment which may noticeably increase its total cost. Furthermore, the use of energy storage devices is important to store the surplus energy and to power these remediation technologies overnight.

In light of the previous studies the modeling and prediction of those treatments are key to understand in detail the behavior of these technologies working under non-constant operational conditions and to assess the level of removal under different weather conditions and consequently a fluctuating powering. Despite the research community has developed mathematical correlations capable of predicting the performance of those remediation technologies under different soft and constant operational conditions and a wide range of pollutants [19-29], there are not literature evidence of studies under realistic conditions (direct coupling with renewable energies). Regarding the green energy storage, a wide range of chemical, mechanical, electromagnetic, thermal or electrochemical systems have been studied in the last centuries [30]. Traditionally, lead-acid and lithium batteries have been widely used to large-scale energy storage acting as buffer between

renewable energy production and a particular energy demand. Nevertheless, the redox flow batteries (RFBs) have shown promising results for large scale requirements between 10 kW and 10 MW due to their flexibility, fast response, depth of discharge and relatively low environmental impact [31, 32]. In addition, the decoupling of power and energy allow the assembly of different configurations that make easier their coupling with renewable energies and other electrochemical devices [33-35]. Until now, many research groups have focused their studies on developing mathematical models capable of predicting the behavior of those energy storage systems, based on the main mechanisms that take place during the charge and discharge steps [36-43].

In view of the previous statements, the main aim of this work is the development of a software tool capable of forecasting the most sustainable and efficient photovoltaic solar electrochemical oxidation treatment assisted by energy storage systems. To do that, simple and pragmatic models interconnected to each other allow to manage the energy coming from photovoltaic (PV) panels in order to exploit the total solar power generated and to reach the maximum remediation during the treatment of a polluted wastewater. To increase and improve the use of energy, a vanadium redox flow battery was used as electrochemical energy storage system which stores exceeding energy and powers an electrochemical remediation treatment at non-power green production hours. To meet this goal, firstly the modeling of the different devices that made up the setup was addressed. Thus, this work exposes for the first time, mathematical models capable of predicting the behavior and performance of electrochemical technologies (an electrooxidation treatment and a redox flow battery) working under hard, intermittent and unpredictable conditions due to their solar powering. After that, the solar power production control and management were faced up to find the most suitable electrical configuration that allows to reach the maximum pollutant mineralization at the maximum removal efficiency.

2. Materials and methods

To validate the different model proposed, experimental tests were performed with different setups. To supply solar photovoltaic energy, two photovoltaic panels model A-160M-24V provided by ATERSA (Spain) were located on the roof of the lab building (3.59N 3.55O). Connection between both panels was in parallel and further details are provided elsewhere [44].

The energy produced by the solar panels aims to be completely exploited by means of an exhaustive control. To do that, it is essential to assess the electrical features of the electrochemical devices that will be powered by them. Furthermore, it is necessary to evaluate the performance of those systems when they are powered by a non-constant power source as the solar energy. To address this aim, the behaviors of a conductive diamond electrochemical oxidation (CDEO) reactor and a vanadium redox flow battery (VRFB) stack working under different operational conditions were assessed. The CDEO reactor used to carry out the experimental tests and the modeling was a DiaCell® 101. The electrochemical reactor was equipped with BDD electrodes (WaterDiam, France) of 78.5 cm^2 of area and connected to a wastewater storage tank as detailed elsewhere [16]. To perform the remediation tests, a synthetic effluent polluted by 100 mg dm^{-3} of an organochlorinated pesticide (Clopyralid) and containing 3000 mg dm^{-3} Na_2SO_4 as supporting electrolyte was used.

Regarding the VRFB stack, a homemade battery of 48 cm^2 each cell was used as energy storage device. A commercial solution of 1.6 M of V^{+n} (50:50 VO^{2+} and V^{3+}), 2 M of H_2SO_4 and 0.05M of H_3PO_4 (OXKEM) was used as electrolyte. Carbon soft felt electrodes Sigracell ® GFA 6 EA (6 mm Thickness) were used as cathode and anode (SGL Group) and Nafion® 117 as cationic exchange membrane (DuPont, Spain).

The complete system was arranged so that the CDEO reactor could be powered by the RFB stack overnight (once the PV could not supply energy). Figure 1 shows a schematic diagram that represents the total remediation system. Because of that, the number of cells contained in the stack were fitted to outperform the electrical requirements of the electrolyzer. To meet this aim, a previous study was carried out which indicated the necessity of connecting 4 cells in series.

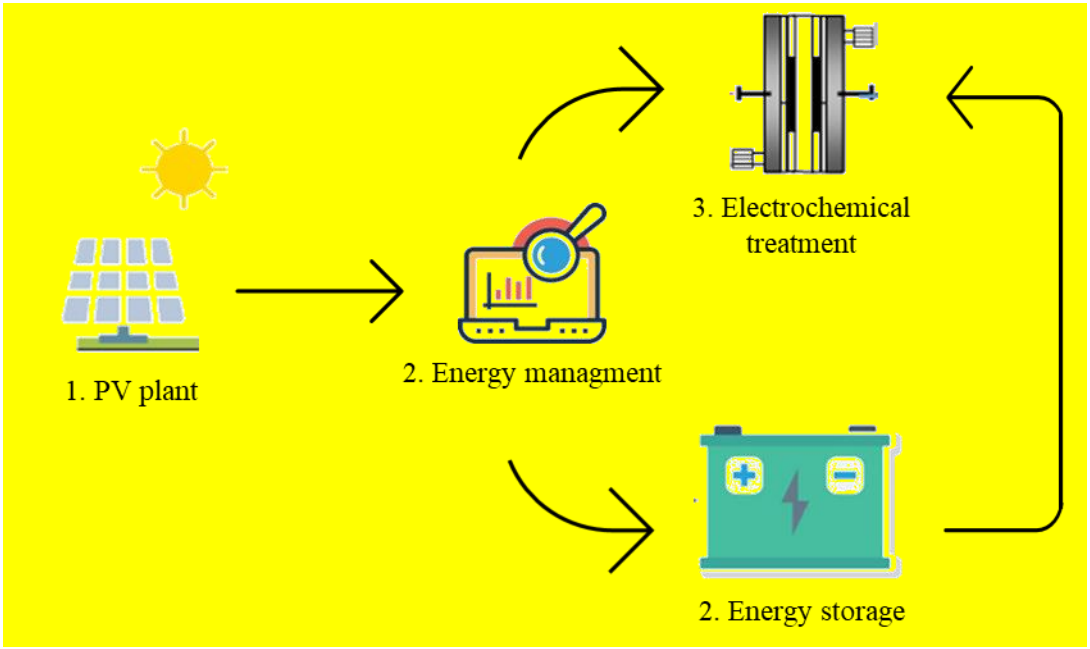

Figure 1. Schematic diagram of a photovoltaic solar electrochemical oxidation treatment assisted by a redox follow battery.

Mathematical models and results discussion

In a previous work, a preliminary approach of a software tool capable of predicting the remediation of an organic compound by means of solar power was developed [44]. That software tool was made up of four modules and it is the base of the work presented in this paper. The first module predicted the solar radiation. The second determined and managed the solar power generated by the PV plant. Finally, the third and fourth modules

were focused on the environmental remediation treatment and the energy storage setups, respectively.

As noticed above, a previous study of our group developed a pragmatic and straightforward model capable of predicting the solar radiation and the energy produced by a PV plant in a specific location [44]. The promising results reached in this first forecast approach set up a new and detailed research path. Thus, this work is mainly focused on improving the second module of the software tool, relied on managing, controlling, and distributing the energy provided by a PV plant. To do that, an exhaustive modelling of the electrochemical devices (remediation treatment and energy storage system) and the solar plant was carried out.

PV panel model. Firstly, an important aspect to be considered is the modelling of the power generated by the PV plant according to the solar radiation received. Once known this input, its management may be faced. Many researchers have focused their studies on the development of different correlations to represent the I-V curves of a photovoltaic panel, depending on the cell temperature, shading, solar radiation or different cell configurations (series or parallel), etc [45, 46]. Most of them expose the behavior of a photovoltaic cell like a diode. Thus, Figure 2 and Equation 1 show the electrical equivalent circuit and the characteristic I-V equation of a photovoltaic panel, respectively [45, 47]. To simplify this part of the modelling tool, the following widely used and accurate model has been used to quantify the solar power generated by our PV plant according to the solar radiation received.

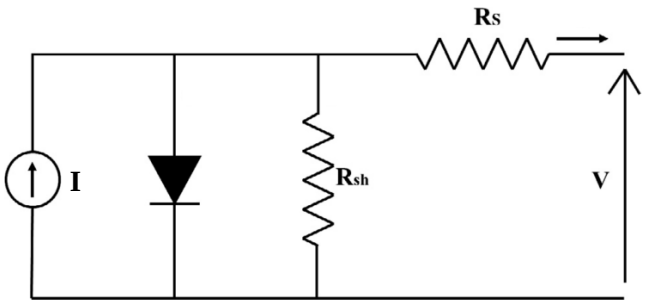

Figure 2. PV cell electrical equivalent circuit.

$$I_{PV} = I_{ph} - I_s \cdot \left[e^{\frac{q \cdot (V_{PV} + I_{PV} \cdot R_s)}{N_c \cdot n \cdot K \cdot T}} - 1 \right] - \frac{V_{PV} + I_{PV} \cdot R_s}{R_{sh}} \quad [1]$$

where, V_{PV} and I_{PV} are the output voltage and current of the PV module. I_{ph} and I_0 are the photocurrent and the inverse saturation current of the diode, respectively. Parameter q is the charge of an electron ($2.6 \cdot 10^{-19}$ C), N_C the number of cells, n is the ideality factor (1.7), K is the Boltzmann constant ($1.3805 \cdot 10^{-23}$ J K^{-1}) and T is the panel temperature. Besides, R_s and R_{sh} represent the series and shunt resistances (Ω), respectively. To simplify the previous equation, some terms have been summarized according to equation 2.

$$a = \frac{q}{N_c \cdot n \cdot K \cdot T} \quad [2]$$

In addition, the I_{ph} and the Is can be calculated easily from equations 3 to 5 where, I_{SC} is the short circuit current, K_I is the temperature coefficient of I_{SC}, λ the solar radiation, I_{rs} the cell saturation current and E_{GO} is the band gap for silicon (1.22 eV).

$$I_{ph} = I_{SC} + K_I \cdot (T - 298) \cdot \frac{\lambda}{1000} \quad [3]$$

$$I_s = I_{rs} \cdot \left(\frac{T}{298} \right)^3 \cdot e^{\frac{q \cdot E_{GO}}{n \cdot K} \cdot \left(\frac{1}{298} - \frac{1}{T} \right)} \quad [4]$$

$$I_{rs} = \frac{I_{SC}}{e^{a \cdot V_{oc}} - e^{I_{SC} \cdot R_s}} \quad [5]$$

To predict the power generated by our solar panels at different solar radiation and temperatures, Equation 1 was adjusted using real data from Atersa (Spain). Figure 3 shows the theoretical and experimental current-voltage curves for a single solar panel model A-160M-24V. The series and shunt resistances were adjusted and took values of 0.379 and 1000 Ω, respectively. Those values are closer to other reported in literature for PV panels with similar characteristics [48-50]. To test the accuracy of the model, theoretical versus experimental current data were fitted, attaining a correlation coefficient of 0.998 which claims the robustness of the selected model to predict the current-voltage curve of a solar panel.

Theoretically, the higher is the solar radiation, the higher is the current supplied by the panel. Conversely, the higher is the temperature of the PV module, the lower is the voltage. Consequently, the higher is the solar radiation and the lower is the solar panel temperature, the higher is the power generated by the PV plant until reaching its maximum power [51, 52]. Considering those facts, if higher voltage or current values are required, additional panels must be connected in series or parallel, respectively.

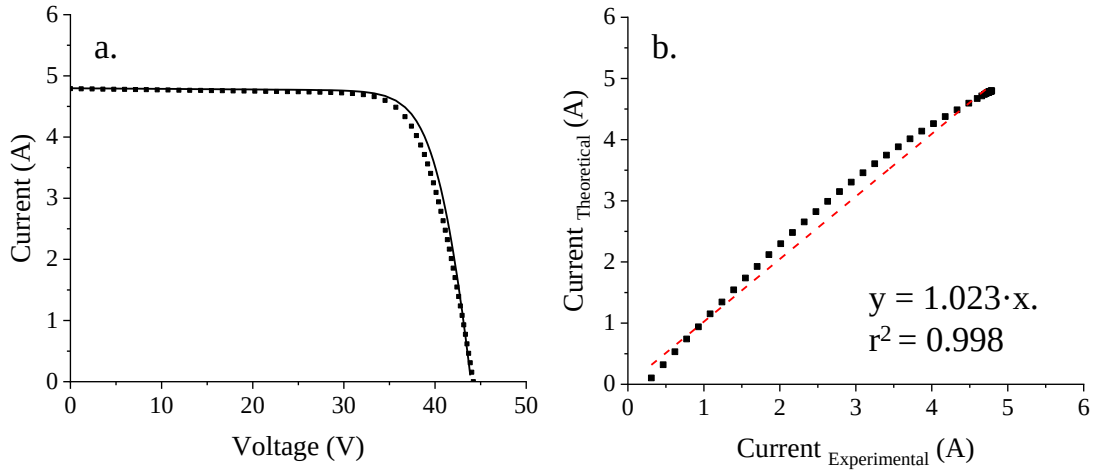

Figure 3. (a) Experimental (■) and theoretical (solid line) current-voltage solar panel curve. (b) Theoretical vs experimental current. Solar panel model: A-160M-24V (Atersa). λ = 1000 W m^{-2}, T_{module}= 25 ºC and N_C = 72.

Despite maximum power does not depend on the connection between the panels, the maximum power current (I_{mp}) and voltage (V_{mp}) values are different in each case. According to the experimental PV plant used in this study made up of two solar panels, the total current that may be supplied by our experimental setup will be the double of a single panel because of the parallel connection between both panels. Conversely, the total voltage will keep constant despite increasing the number of cells.

From these results, the power generated by a PV plant regarding a specific solar radiation can be predicted. Nevertheless, the supplied voltage and current depend on the electrical features of the devices directly connected to them. In this specific case, a CDEO and a RFB stack will be powered by renewable energy. To quantify the energy supplied by the PV plant in a punctual and specific moment of the day, the current-voltage curves of the coupled devices must be modelled and validated using experimental data.

Model of Electrochemical cells. The cell potential (E_{cell}) of an electrochemical device is defined by the equilibrium potential (E_{eq}) and the overpotentials (η) [53], as equation 6 shows, where η_{ohm}, η_{act} and η_{con} are the ohmic, activation and concentration overpotentials, respectively. On the other hand, the current is governed by the rate of several reaction such as mass transfer from the bulk solution to the electrode surface, the electron transfer at the electrode surface and chemical reactions on the electrode surface [54],

$$E_{cell} = E_{eq} \pm (\eta_{ohm} + \eta_{act} + \eta_{con}) \quad [6]$$

The equilibrium potential is defined by Nernst equation (equation 7) and depends on the standard potential (E^0) of the half reactions that take place in each electrode and the concentration of species [55], where, R is the gas constant (8.31 J mol^{-1} K^{-1}), T is the temperature in Kelvin, F is the Faraday constant (96485.33 C mol^{-1}) and n is the number

of electrons transferred. Besides, and [Red] and [Ox] represent the concentrations of reductant oxidant species, respectively (mol dm^{-3}).

$$E_{eq}=E^0 - \frac{R\cdot T}{F\cdot n}\cdot \ln\left(\frac{[Red]}{[Ox]}\right) \quad [7]$$

Regarding overpotentials, different losses may appear when an electrochemical reaction takes place due to operational limitations. Ohmic overpotentials are related to the internal resistance of the electrochemical device (R_{ohm}) and this is mainly due to the ionic resistance of the electrolyte, the electrical resistance of the electrode and the current collector, and the contact between them [56]. The ohmic overpotential may be expressed by the following expression and it directly depends on the current (I) supplied to the system.

$$\eta_{ohm}= R_{ohm}\cdot I \quad [8]$$

One the other hand, charge and mass transfer limitations may arise when electrons or reactants have "difficulties" to reach the electrode surface [57], respectively. Concerning activation overpotentials, to quantify these losses during an electrochemical process free of mass transfer limitation, the well-known Butler-Volmer equation is used [55], equation 9. This equation can be drawn as equation 10 to represent the activation overpotential of the anodic and cathodic electrode, first and second part of this expression, respectively, where α corresponds to the transfer coefficient and I_0 with the exchange current (A).

$$I = I_0 \cdot \left[e^{-\alpha\cdot\frac{F}{R\cdot T}\cdot\eta} - e^{(1-\alpha)\cdot\frac{F}{R\cdot T}\cdot\eta}\right] \quad [9]$$

$$\eta_{act}=\frac{RT}{F\cdot n}\cdot\left[\frac{1}{(1-\alpha)}\cdot(\ln(I) - \ln(I_0) - \frac{1}{\alpha}\cdot(\ln(I) - \ln(I_0)\right] \quad [10]$$

Several assumptions may be considered according to the range of operational overpotential. At lower overpotential, the electrode is highly cathodically polarized and

consequently, the first term of equation 9 may be got rid of. Conversely, at higher overpotentials, the cathodic component may be zero. Regarding concentration overpotentials (Equation 11), these may appear at lower reactant concentration because of the concentration on the electrode surface is not enough to promote the electrochemical reaction. In turn, non-desirable reactions and higher wasted energy consumption may take place because of exceeded current densities [58, 59], where, k_m is the mass transfer coefficient (dm s^{-1}), C is the reagent concentration (mol dm^{-3}) and A is the electrode area (m^2).

$$\eta_{con} = \frac{RT}{Fn} \cdot \left(1 - \frac{I}{F \cdot A \cdot km \cdot C}\right) \quad [11]$$

Given the complexity of the previous equations and the widely and variable concentration of intermediates species that may appear in the bulk solution during an electrooxidation treatment according to the degradation pathway of a pollutant, the current-voltage curve of the CDEO reactor was simplified, as Equation 12 shown. In this case, the parameters *a* and *b* represent the equilibrium potential and the electrode overpotentials, respectively. Otherwise, *c* corresponds with ohmic resistance directly related to the cells design and the conductivity of the electrolyte as aforementioned.

$$E_{cell} = a + b \cdot \ln(I) + c \cdot I \quad [12]$$

Conversely, the current-voltage curve of the RFB was adjusted considering the above equations. It is worth mentioning that the overpotentials are added to the E_{eq} for the charge process. In contrast, those terms are subtracted from E_{eq} during the discharge step [38].

Furthermore, some additional assumptions were considered to quantify the overpotentials at each moment of the process. To determine if the process is going to suffer charge or mass transferer limitation, the punctual current and reagent concentration was compared to the punctual current (I_{lim}) and concentration (C_{lim}) limits, respectively. Equations 13

and 14 show the expressions to estimate the current and concentration limits, respectively. Thus, if the current supplied to the systems is lower than the current limit ($I < I_{lim}$), the activation overpotential will arise. On the other hand, if the concentration of reagent is lower than the limit reagent concentration ($C < C_{lim}$), the electrochemical process will be mass transfer limited and the effect of the concentration overpotential will be considered. As detailed previously, k_m is the mass transfer coefficient and its value for the homemade RFB stack used in this work was estimated by the following empirical, equation 15 [60], where, in turn, Q the flow rate ($dm^3\ s^{-1}$) and *h* and *w* are the thickness and width of the electrode (dm), respectively.

$$I_{limit}\ (t) = n \cdot F \cdot A \cdot k_m \cdot C\ (t) \qquad [13]$$

$$C_{limit}\ (t) = \frac{I\ (t)}{n \cdot F \cdot k_m} \qquad [14]$$

$$k_m = 1.6 \cdot 10^{-4} \cdot \left(\frac{Q}{h \cdot w}\right)^{0.4} \qquad [15]$$

It is important to note that the concentration of reagent (C) will be different according to the half cell and to the charge-discharge step [38, 61]. Thus, for the negative half-cell, C will be referred to the V^{+3} and V^{+2} concentrations during the charge and discharge cycles, respectively. Conversely, C will be tied to the V^{+4} and V^{+5} concentration in the charge and discharge steps, respectively.

Electric integration of the solar panel to the electrolyzer models. Considering these premises, the current-voltage curves of the CDEO cell and the RFB stack were modelled. An important aspect to be considered is that in contrast to a traditional modelling, this study allows to assess the behaviour of these electrochemical devices powered by a PV panel and not at galvanostatic mode. Once known the solar radiation received in a located place in a specific time, it can be quantified the amount of energy that will be supplied to

each single device. Figure 4 shows the current and voltage supplied to each electrochemical device when they are directly connected to specific PV panels. Theoretical values follow the same trend than the experimental one. Slight differences can be observed in all cases between both values. Those differences may be due to the fluctuating powering performed by the PV panels. Experimental data were recorded for a shorter period which turns into a more variable signal. Those fluctuations may be related to punctual shading on the PV panel surface, because of the cloud cover that may drop the power generated. Current and voltage values were recorded throughout a day for the CDEO reactor. In contrast, for the RFB, these values were recorded until the full state of charge of the battery. The battery is completely charged when the cell voltage reaches 7.2 V (cut-off voltage).

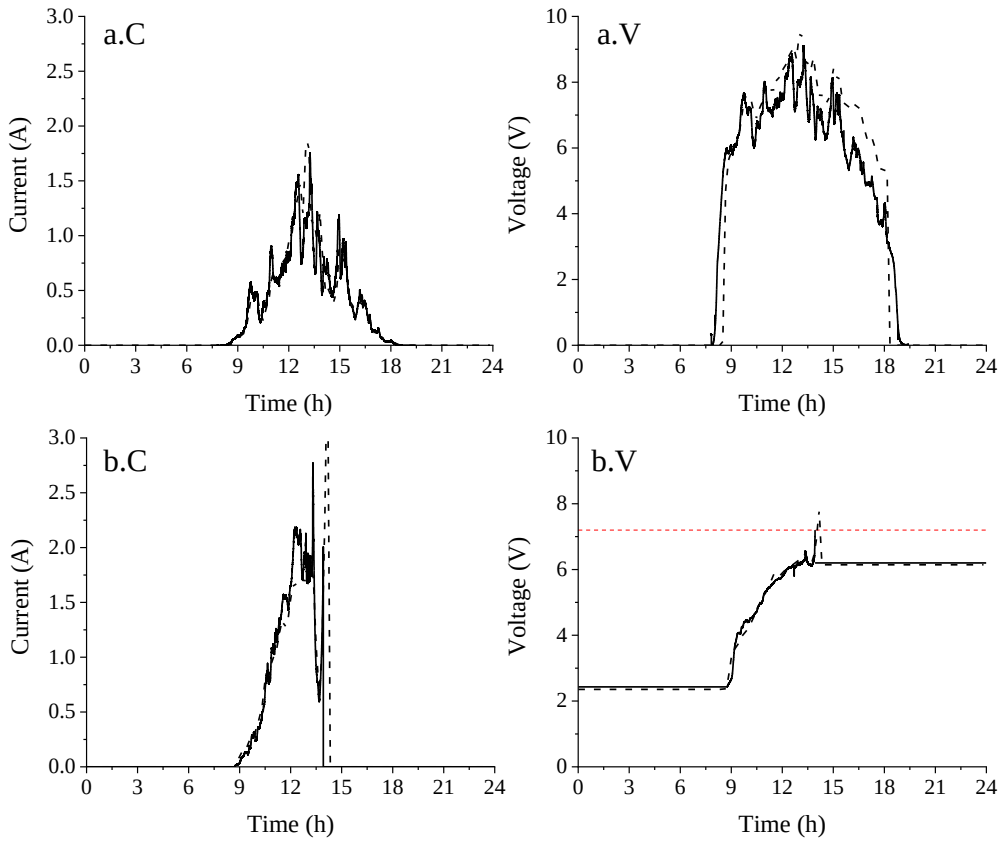

Figure 4. Current (C) and voltage (V) values supplied to the CDEO (a) and the RFB stack (b) by the PV plant. Experimental (solid line) and theoretical (dashed line) data. Red

dashed line: Cut off voltage value at charge step, 7.2 V. RFB electrolyte volume = 0.5 dm^3; Initial concentration of vanadium = 1.6 mol dm^{-3}.

To evaluate the accuracy of the proposed model to predict the energy supplied by a PV plant to power the CDEO cell and the RFB stack, theoretical vs experimental data were fitted. Figure 5 shows the fitting plots for the voltage and current values of both electrochemical devices. Furthermore, correlation coefficients were calculated to estimate the deviation of the theoretical values regarding the experimental one. Due to the higher precision of experimental data because of the large values recorded, the punctual values may differ from the theoretical one calculated by a shorter period. Considering this fact, the fittings were assessed by different periods of time through quadratic means.

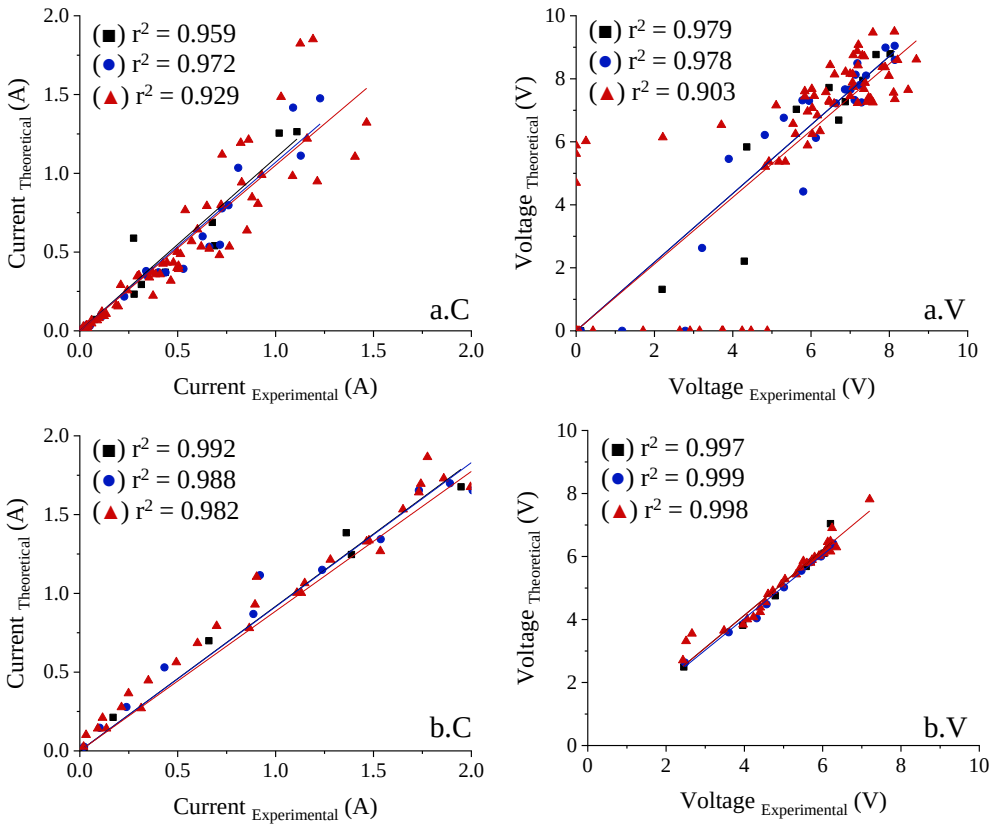

Figure 5. Experimental vs theoretical current (C) and voltage (V) data. Energy supplied from a PV plant to the CDEO (a) or the RFB stack (b). Average values of 60 min (■), average value of 30 min (●) and punctual value (▲).

As expected, the fittings performed by the punctual values of current or voltage showed lower correlation coefficients. Conversely, the higher is the operational period tested, the higher is the accuracy of the model to predict the energy supplied by the PV plant. Nevertheless, despite the lower precision reached by the model in a given moment, the correlation coefficients were higher than 0.98 in all cases. Thus, those results confirm the robustness and reliability of the model to predict the powering of a CDEO reactor and a RFB stack by a PV plant. On the other hand, it is important to point out that the Open Circuit Potential (OCP) of the stack is highly precise despite the Nernst equation does not include the term of concentration of protons. Many researchers have included the Donnan potential to the Nernst term to increase the precision of the model and predict the unbalanced proton concentration between the two compartments of the battery [42] but, as the results demonstrate, in our approach it is not necessary.

Electric integration of the RBD discharge and the CDEO models. Keeping in mind that the RFB stack will be used as booster of the environmental remediation treatment, its coupling must be assessed. Consequently, it was evaluated the discharge current-voltage curve of the RFB stack when this energy storage system is used as power source of a CDEO reactor. As aforementioned, the current-voltage curve was modelled by means of equation 6. In contrast to the expression that represents the charge curve, the overpotentials were subtracted from the equivalent potential.

One of the strengths of the redox flow batteries is the independent sizing of power and energy [34, 62, 63]. Thus, the number of cells that makes up a stack must be enough to overcome the overpotentials offered by the battery and the electrochemical device that will be powered by it. Previous studies determined the minimum number of cells that must make up the RFB stack to power the specific CDEO reactor as 4 cells.

On the other hand, the capacity of the battery is determined by the volume of electrolyte [64, 65]. Consequently, given a discharge current value, the volume of electrolyte must be optimized to get a desired discharge time.

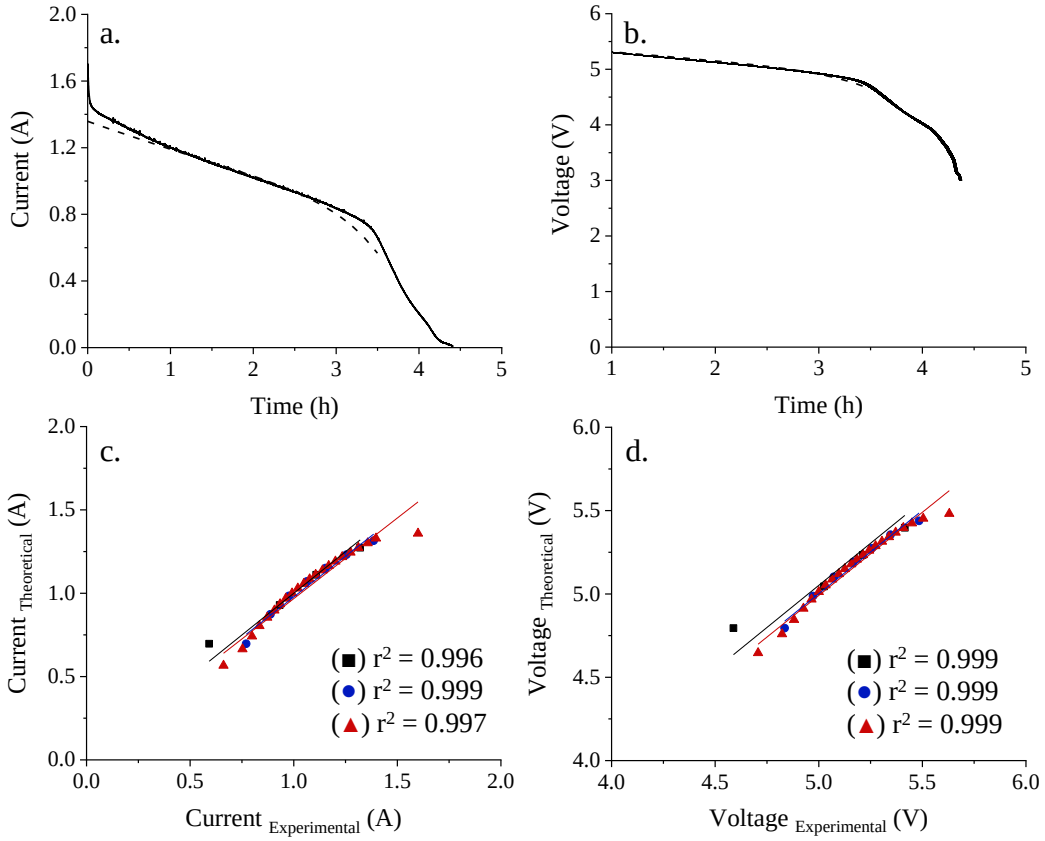

s

Figure 6. Current and voltage values supplied to a EAOP (a) and a RFB stack (b) by a PV plant. Experimental (solid line) and theoretical (dished line) data. Experimental vs theoretical current (c) and voltage (d) values. Average values of 60 min (■), average value of 30 min (●) and punctual value (▲).

To compare in equal terms, the modelling of the current-voltage discharge curve of the battery the same experimental charge-discharge cycle was used. Once the battery reached the full state of charge, it was directly coupled to the CDEO reactor to assess its discharge. Figure 6 shows the experimental and theoretical current and voltage supplied by the RFB stack to the EAOP. As in previous cases, theoretical versus experimental data were confronted and fitted with the aim of quantifying the accuracy of the model. In agreement

with the Figure 6 a and b, the fittings showed higher correlation coefficients which confirm the huge exactitude of the model to predict the distribution of energy between two electrochemical devices. Thus, results suggest once again that the model predicts in a high level of precision and robustness the energy supplied by a RFB stack.

In order to quantify in a higher level of detail the performance of the redox flow battery working under realistic conditions, the electrical features of the charge-discharge steps were assessed. Supplementary Material reports the experimental and theoretical capacities and energies reached by the RFB.

Once proved that PV panels are capable of working as power source of a PSEO and a RFB and considering that the RFB may operate as energy booster of the electrooxidation treatment, it its essential to evaluate the influence of an intermittent powering on the performance of an electrochemical remediation treatment to clean up a wastewater effluent.

Decontamination model. As noticed previously, the main aim of this work is to predict and quantify the level of degradation that may reach a polluted effluent after a photovoltaic solar electrochemical oxidation (PSEO) treatment assisted by an RFB. Considering this premise, the drop of pollutant during an electrooxidation treatment working under different operation modes was addressed.

Until now, the performances of electrooxidation treatments have been widely study in literature under galvanostatic condition. In contrast to that, the coupling of those technologies with a renewable energy brings out a harder and variable powering. Thus, this work reports for the first time a model able to predict the remediation trend of an electrooxidation treatment running under realistic conditions by means of a solar powering. Keeping in mind previous modelling studies, Panizza et al. [66] developed a

theoretical model able to predict the chemical oxygen demand (COD) and the instantaneous current efficiency (ICE) under an electrooxidation treatment performed on batch mode working with BDD electrodes. The application of this model has some particularities depending on the operation mode and the species involved in the reaction. Two regimens were distinguished depending on the dominant control of the electrolysis process, current control or mass transport control [19, 20, 67-69]. Thus, the removal rate of the process depends on α, constant that relates the applied and limited current (I_{lim}, Equation 13). Consequently, α values lower than 1 correspond to a process working under current control regimen. Conversely, values of α over 1 are directly related to mass transfer-controlled processes. Equations 16 and 17 represent the mathematical expressions that describe the kinetic model of the remediation treatment working under current or mass transfer control regime, respectively, where [POP] corresponds to the concentration of persistent organic pollutant (mg dm^{-3}), t is the treatment time (h), and V_R is the reactor volume (dm^3).

$$[POP]\,(t) = [POP]_0 \cdot \left(1 - \frac{\alpha \cdot A \cdot k_m}{V_R} \cdot t\right) \quad [16]$$

$$[POP]\,(t) = \alpha \cdot [POP]_0 \cdot \exp\left(- \frac{A \cdot k_m}{V_R} \cdot t + \frac{1 - \alpha}{\alpha}\right) \quad [17]$$

Those equations have been widely used by many other research groups to model the mineralization of different organic compounds [21, 24, 25, 27]. Nevertheless, to the best of our knowledge the modelling of electrolysis treatment has not been performed under non-galvanostatic conditions. As outlined, this work seeks to evaluate the degradation and performance of a PSEO treatment. Consequently, the operational regime may vary throughout the treatment according to the current supplied by the PV plant as a function of the solar radiation received. Thus, the removal of clopyralid under batch mode was

evaluated at galvanostatic and non-galvanostatic modes according to the regimes described above.

Furthermore, it is important to keep in mind that the water treatment plants work at continuous mode. For this reason, the PSEO of clopyralid was also evaluated under this operational flow mode. To test the kinetic model of an environmental remediation treatment working under continuous mode, the same regimes exposed before were considered for a comparative proposed.

- $\alpha < 1$: Electrooxidation under current limited control
- $\alpha > 1$: Electrooxidation under mass transport control

According to this theoretical approach, the kinetic model of a continuous electrooxidation treatment was adjusted by means of equation 18 which represents a mass balance. Because of the treatment works as continuous mode, a constant inlet and outlet stream come in and out to the reactor. Furthermore, the generation term has a negative reaction due to the organic matter presented into the water body will be removed and there is no matter generation. Considering those facts, equation 18 can be drawn as equation 19, where q_v is the volumetric flow ($dm^3\ h^{-1}$). The reaction term (r) of a direct electrochemical process directly depends on the current applied and the number of electrons transferred by equation 20. Likewise, remediation efficiency is set by the parameter Eff as function of the parameter α [66], as equation 21 shows.

$$[Acumulation] = [Inlet] - [Outlet] + [Generation] \quad [18]$$

$$\frac{V_R \cdot d[POP]_t}{dt} = q_v \cdot [POP]_0 - q_v \cdot [POP]_t - r \quad [19]$$

$$r = \frac{I}{n \cdot F} \quad [20]$$

$$Eff = \frac{[POP]_t}{\alpha \cdot [POP]_0} \quad [21]$$

In view of the previous statements equation 20 can be drawn as follow to model the kinetic degradation of an organic pollutant by a continuous electrooxidation treatment.

$$[POP]_t = [POP]_{t-1} + \frac{t - t_0}{V_R} \cdot \left[q_v \cdot \left([POP]_{t_0} - [POP]_{t-1} \right) - \frac{I}{n \cdot F} \cdot Eff \right] \quad [23]$$

In the light of the previous theoretical approaches, the modelling of clopyralid electrooxidation working under batch and continuous mode and powered at galvanostatic and non-galvanostatic mode was addressed. The number of electrons exchanged during the electrolysis of clopyralid were set up at 18 according to reaction 1.

$$C_6H_3Cl_2NO_2 + 10H_2O \rightarrow 6CO_2 + 19H^+ + NH_4^+ + 2Cl^- + 18\ e^- \quad (1)$$

Figure 7 shows the theoretical and experimental clopyralid drop for each of the aforementioned cases of study. As in previous cases, experimental versus theoretical data were fitted with the aim of evaluating the accuracy of the proposed model to predict the clopyralid mineralization under different electrooxidation conditions. The mineralization of clopyralid in batch mode was modelled at two different current densities, 10 and 100 mA cm^{-2} to assess the removal trend under different operational regimes.

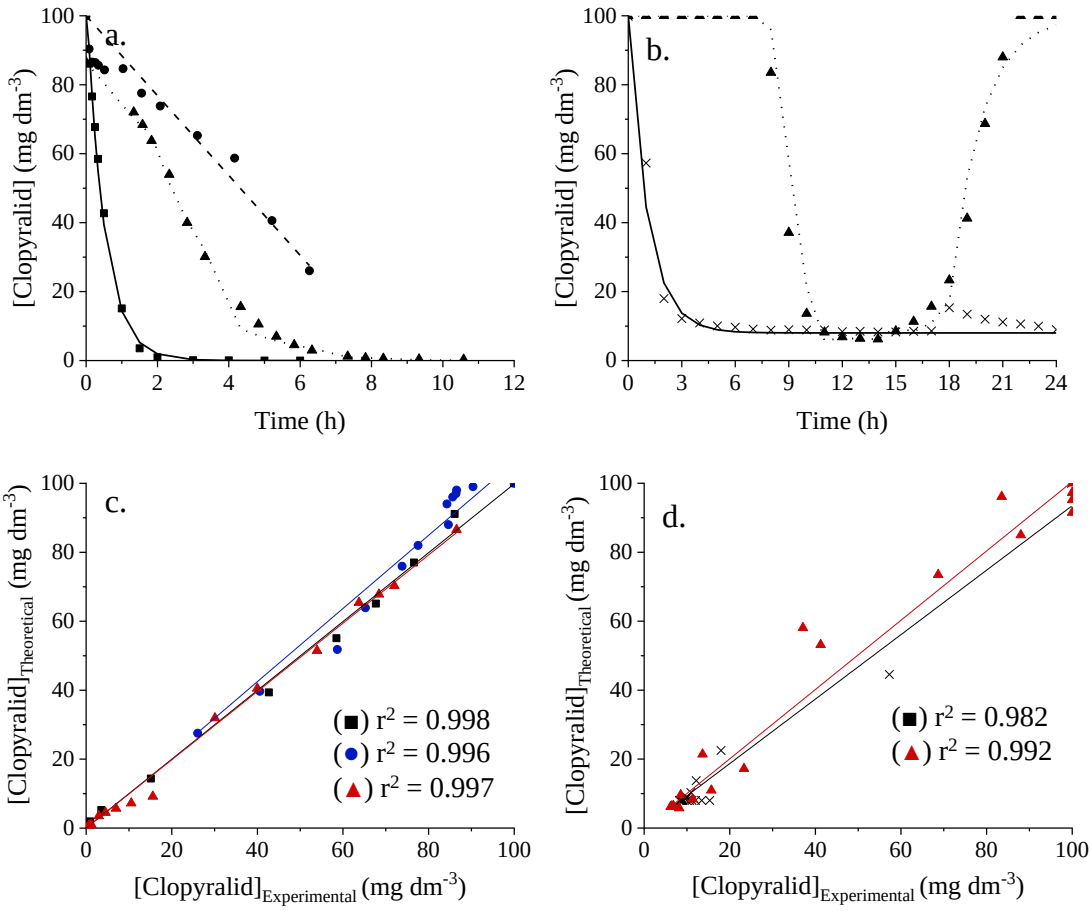

460

461 **Figure 7.** Removal of clopyralid under discontinuous (a) and discontinuous (b)
462 electrooxidation treatments working at galvanostatic mode (■ 100 mA cm^{-2}, ● 10 mA cm^{-2} and x 16.3 mA cm^{-2}) and at non-constant current density by means of a solar powering
463 (▲). Experimental vs theoretical clopyralid concentration under discontinuous (c) and
464 continuous (d) operational mode. $[Clop]_0$ = 100 mg dm^{-3}; $K_m = 2.8 \cdot 10^{-6}$ m s^{-1}; A 78.5
465 cm^2; V_R = 0.039 dm^3; q_V = 0.0852 dm^3 h^{-1}.

466

467 As Figure 7 shows, the electrooxidation carried out at 100 mA cm^{-2} follows a mass
468 transport control regime. Conversely, the environmental remediation treatment developed
469 at 10 mA cm^{-2} works under a current control regime. α was adjusted by each case and
470 took values of 1.51 and 0.057, respectively. On the other hand, the electrolysis treatment
471 working under a solar powering may run under a mass or a current control regimen. Low
472 current densities bring out charge transfer limitation. In contrast to that, a low

concentration of pesticides sheds light of mass transfer problems because the specie of interest will not be able to reach the electrode surface to be oxidized. In this way, α varied along the experimental treatment according to the concentration of pollutant remained into the bulk solution and the current supplied by the PV panel. Figure 7 c shows the experimental versus theoretical results. The fittings and correlation coefficients notice a huge level of precision of the model to predict the removal of clopyralid at galvanostatic and non-galvanostatic mode when the reactor is fed in batch mode. In agreement with the results reached in batch mode, the model proposed to forecast the remediation of clopyralid under continuous mode showed also promising results. As expected, the degradation of pesticide under PSEO reveals an increase of removal until the peak hour. After that, a drop of efficiency is observed in the afternoon due to the lower solar radiation received at this period of the day. Furthermore, it can be seen that the remediation is nil at night due to the solar panel is not able to produce energy because of solar radiation is not received. Nevertheless, the model predicts the mineralization trend in a high level of accuracy, reporting a correlation coefficient of 0.992, slightly higher than the value observed at galvanostatic mode.

In short, the data summarized in this section claims that the proposed model predicts the remediation trend of an electrooxidation treatment working under realistic conditions, non-galvanostatic conditions and continuous flow mode.

3. Conclusions

This work reports the modelling of a solar photovoltaic solar electrochemical oxidation assisted by a redox flow battery stack. Result pointed out that simple pragmatic models can be used to understand the effect of a non-continuous power supply on the performance of electrochemical devices, PSEO and RFB. Furthermore, those models claim that the production of energy of a PV panel can be predicted once known the solar radiation

498 received in a located place and a specific time and the energy supplied by the solar panel
499 to each electrochemical device can be estimated with a huge level of robustness thanks to
500 the curves current – voltage of systems devices. Thus, this energy must be distributed
501 after its exhaustive prediction in order to undertake the most sustainable and efficient
502 PSEO. The degradation of clopyralid has been modelled under different flow and
503 powering operational conditions, showing in all cases a high level of accuracy and
504 robustness to predict the mineralization of clopyralid. In addition, results confirm that the
505 RFB is one of the most flexible energy storage systems. This battery can be designed
506 according to the electrical features of the system that is going to be stored and can work
507 as electrical booster of an PSEO at low or null power production hours. In short, the use
508 of a predictive software tool allows to estimate and control the energy produced by a PV
509 plant in order to develop the most efficient and sustainable remediation treatment.

510 **Acknowledgments**

511 Financial support from the Spanish Agencia Estatal de Investigación through project
512 PID2019-107271RB-I00 (AEI/FEDER, UE) is gratefully acknowledged. M. Millán
513 thanks the UCLM for the predoctoral contract within the framework of the Plan Propio
514 I+D.

515 **References**

516 [1] L.J.P. Snip, X. Flores-Alsina, B.G. Plósz, U. Jeppsson, K.V. Gernaey, Modelling the
517 occurrence, transport and fate of pharmaceuticals in wastewater systems, Environ.
518 Modell. Softw., 62 (2014) 112-127.
519 [2] A.W. da S Trentin, K.R. Reddy, G. Kumar, J.K. Chetri, A. Thomé, Quantitative
520 Assessment of Life Cycle Sustainability (QUALICS): Framework and its application to
521 assess electrokinetic remediation, Chemosphere, 230 (2019) 92-106.

[3] J.F.J.R. Pesqueira, M.F.R. Pereira, A.M.T. Silva, Environmental impact assessment of advanced urban wastewater treatment technologies for the removal of priority substances and contaminants of emerging concern: A review, J. Clean. Prod., 261 (2020).
[4] M. Al-Obaidi, C. Kara-Zaitri, I.M. Mujtaba, Wastewater Treatment by Reverse Osmosis Process: State of the Art & Process Modelling, CRC Press2020.
[5] S.M. Moni, R. Mahmud, K. High, M. Carbajales-Dale, Life cycle assessment of emerging technologies: A review, J. Ind. Ecol., 24 (2020) 52-63.
[6] M.A. Rodrigo, N. Oturan, M.A. Oturan, Electrochemically Assisted Remediation of Pesticides in Soils and Water: A Review, Chem. Rev., 114 (2014) 8720-8745.
[7] P.V. Nidheesh, M. Zhou, M.A. Oturan, An overview on the removal of synthetic dyes from water by electrochemical advanced oxidation processes, Chemosphere, 197 (2018) 210-227.
[8] M.A. Oturan, J.-J. Aaron, Advanced Oxidation Processes in Water/Wastewater Treatment: Principles and Applications. A Review, Crit. Rev. Env. Sci. Technol., 44 (2014) 2577-2641.
[9] S. Ahmadzadeh, M. Dolatabadi, In situ generation of hydroxyl radical for efficient degradation of 2,4-dichlorophenol from aqueous solutions, Environ. Monit. Assess., 190 (2018) 340.
[10] M. Dolatabadi, S. Ahmadzadeh, M.T. Ghaneian, Mineralization of mefenamic acid from hospital wastewater using electro-Fenton degradation: Optimization and identification of removal mechanism issues, Environmental Progress & Sustainable Energy, 39 (2020) e13380.
[11] Y. Abdollahi, A.H. Abdullah, U.I. Gaya, S. Ahmadzadeh, A. Zakaria, K. Shameli, Z. Zainal, H. Jahangirian, N.A. Yusof, Photocatalytic degradation of 1,4-benzoquinone in aqueous ZnO dispersions, J Brazil Chem. Soc., 23 (2012) 236-240.

547 [12] E. Chatzisymeon, S. Foteinis, D. Mantzavinos, T. Tsoutsos, Life cycle assessment
548 of advanced oxidation processes for olive mill wastewater treatment, J. Clean. Prod., 54
549 (2013) 229-234.
550 [13] C.M. Fernández-Marchante, F.L. Souza, M. Millán, J. Lobato, M.A. Rodrigo,
551 Improving sustainability of electrolytic wastewater treatment processes by green
552 powering, Sci. Total. Environ., 754 (2021).
553 [14] F.L. Souza, C. Saéz, J. Llanos, M.R.V. Lanza, P. Cañizares, M.A. Rodrigo, Solar-
554 powered electrokinetic remediation for the treatment of soil polluted with the herbicide
555 2,4-D, Electrochim. Acta, 190 (2016) 371-377.
556 [15] M. Millán, P.Y. Bucio-Rodríguez, J. Lobato, C.M. Fernández-Marchante, G. Roa-
557 Morales, C. Barrera-Díaz, M.A. Rodrigo, Strategies for powering electrokinetic soil
558 remediation: A way to optimize performance of the environmental technology, J.
559 Environ. Manage., 267 (2020) 110665.
560 [16] M. Millán, M.A. Rodrigo, C.M. Fernández-Marchante, P. Cañizares, J. Lobato,
561 Powering with Solar Energy the Anodic Oxidation of Wastewater Polluted with
562 Pesticides, ACS Sustain. Chem. Eng., 7 (2019) 8303-8309.
563 [17] D. Marmanis, K. Dermentzis, A. Christoforidis, K. Ouzounis, A. Moumtzakis,
564 Electrochemical treatment of actual dye house effluents using electrocoagulation process
565 directly powered by photovoltaic energy, Desalination Water Treat., 56 (2015) 2988-
566 2993.
567 [18] D. Valero, J.M. Ortiz, E. Expósito, V. Montiel, A. Aldaz, Electrocoagulation of a
568 synthetic textile effluent powered by photovoltaic energy without batteries: Direct
569 connection behaviour, Sol. Energy Mater. Sol. Cells, 92 (2008) 291-297.

570 [19] A. Urtiaga, C. Fernández-González, S. Gómez-Lavín, I. Ortiz, Kinetics of the
571 electrochemical mineralization of perfluorooctanoic acid on ultrananocrystalline boron
572 doped conductive diamond electrodes, Chemosphere, 129 (2015) 20-26.
573 [20] O. Scialdone, A. Galia, S. Randazzo, Electrochemical treatment of aqueous solutions
574 containing one or many organic pollutants at boron doped diamond anodes. Theoretical
575 modeling and experimental data, Chem. Eng. J., 183 (2012) 124-134.
576 [21] M. Panizza, A. Kapalka, C. Comninellis, Oxidation of organic pollutants on BDD
577 anodes using modulated current electrolysis, Electrochim. Acta, 53 (2008) 2289-2295.
578 [22] A.M. Polcaro, M. Mascia, S. Palmas, A. Vacca, Kinetic Study on the Removal of
579 Organic Pollutants by an Electrochemical Oxidation Process, Ind. Eng. Chem. Res., 41
580 (2002) 2874-2881.
581 [23] A. Kapałka, G. Fóti, C. Comninellis, Kinetic modeling of the Electrochemical
582 mineralization of organic pollutants for wastewater treatment, J. Appl. Electrochem., 38
583 (2008) 7-16.
584 [24] G. Tissot, A. Anglada, P. Dimitriou-Christidis, L. Rossi, J. Arey, C. Comninellis,
585 Kinetic experiments of electrochemical oxidation of iohexol on BDD electrodes for
586 wastewater treatment, Electrochem. Commun., 23 (2012) 48–51.
587 [25] P. Canizares, J. Garcia-Gomez, J. Lobato, M. Rodrigo, Electrochemical oxidation of
588 aqueous carboxylic acid wastes using diamond thin-film electrodes, Ind. Eng. Chem.
589 Res., 42 (2003) 956-962.
590 [26] L. Gherardini, P.A. Michaud, M. Panizza, C. Comninellis, N. Vatistas,
591 Electrochemical Oxidation of 4-Chlorophenol for Wastewater Treatment: Definition of
592 Normalized Current Efficiency (φ), J. Electrochem. Soc., 148 (2001) D78.

[27] M.A. Rodrigo, P.A. Michaud, I. Duo, M. Panizza, G. Cerisola, C. Comninellis, Oxidation of 4-chlorophenol at boron-doped diamond electrode for wastewater treatment, J. Electrochem. Soc., 148 (2001) D60-D64.

[28] A. Amaral, S. Gillot, M. Garrido-Baserba, A. Filali, A.M. Karpinska, B.G. Plósz, C. De Groot, G. Bellandi, I. Nopens, I. Takács, I. Lizarralde, J.A. Jimenez, J. Fiat, L. Rieger, M. Arnell, M. Andersen, U. Jeppsson, U. Rehman, Y. Fayolle, Y. Amerlinck, D. Rosso, Modelling gas–liquid mass transfer in wastewater treatment: when current knowledge needs to encounter engineering practice and vice versa, Water Sci. Technol., 80 (2019) 607-619.

[29] M. Dolatabadi, M. Mehrabpour, M. Esfandyari, S. Ahmadzadeh, Adsorption of tetracycline antibiotic onto modified zeolite: Experimental investigation and modeling, MethodsX, 7 (2020) 100885.

[30] S. Ould Amrouche, D. Rekioua, T. Rekioua, S. Bacha, Overview of energy storage in renewable energy systems, Int. J. Hydrogen Energy, 41 (2016) 20914-20927.

[31] M. Skyllas-Kazacos, L. Cao, M. Kazacos, N. Kausar, A. Mousa, Vanadium Electrolyte Studies for the Vanadium Redox Battery—A Review, ChemSusChem, 9 (2016) 1521-1543.

[32] P. Leung, X. Li, C. Ponce de León, L. Berlouis, C.T. John Low, F. Walsh, Progress in redox flow batteries, remaining challenges and their applications in energy storage, RSC Adv., 2 (2012) 10125-10156.

[33] T.M. Letcher, Storing Energy: with Special Reference to Renewable Energy Sources, Elsevier Science2016.

[34] W. Wang, Q. Luo, B. Li, X. Wei, L. Li, Z. Yang, Recent Progress in Redox Flow Battery Research and Development, Adv. Funct. Mater., 23 (2012) 970-986.

[35] J. Lobato, E. Mena, M. Millán, Improving a Redox Flow Battery Working under Realistic Conditions by Using of Graphene based Nanofluids, ChemistrySelect, 2 (2017) 8446-8450.

[36] M.M. Seepana, S. Samudrala, P.V. Suresh, R. Vooradi, Unit Cell Modelling and Simulation of All Vanadium Redox Flow Battery, 13 (2017) 20170014.

[37] A.A. Shah, M.J. Watt-Smith, F.C. Walsh, A dynamic performance model for redox-flow batteries involving soluble species, Electrochim. Acta, 53 (2008) 8087-8100.

[38] M. Pugach, M. Kondratenko, S. Briola, A. Bischi, Numerical and experimental study of the flow-by cell for Vanadium Redox Batteries, Energy Procedia, 142 (2017) 3667-3674.

[39] A. Tang, J. Bao, M. Skyllas-Kazacos, Studies on pressure losses and flow rate optimization in vanadium redox flow battery, J. Power Sources, 248 (2014) 154-162.

[40] V. Yu, D. Chen, Dynamic Model of a Vanadium Redox Flow Battery for System Performance Control, Journal of Solar Energy Engineering, 136 (2013) 021005.

[41] S.K. Padavala, A. Sharma, C. Choo, E. Birgersson, Analysis of Concentration Overpotential in an All-Vanadium Redox Flow Battery, J. Electrochem. Soc., 165 (2018).

[42] K.W. Knehr, E.C. Kumbur, Open circuit voltage of vanadium redox flow batteries: Discrepancy between models and experiments, Electrochem. Commun., 13 (2011) 342-345.

[43] M. Skyllas-Kazacos, M. Kazacos, State of charge monitoring methods for vanadium redox flow battery control, J. Power Sources, 196 (2011) 8822-8827.

[44] M. Millán, J. Lobato, P. Cañizares, M.A. Rodrigo, Prediction and management of solar energy to power electrochemical processes for the treatment of wastewater effluents, Electrochim. Acta, 335 (2020).

641 [45] Y. Chaibi, M. Salhi, A. El-jouni, A. Essadki, A new method to extract the equivalent
642 circuit parameters of a photovoltaic panel, Sol. Energy, 163 (2018) 376-386.
643 [46] S. Bana, R.P. Saini, Experimental investigation on power output of different
644 photovoltaic array configurations under uniform and partial shading scenarios, Energy,
645 127 (2017) 438-453.
646 [47] Y.-J. Wang, P.-C. Hsu, An investigation on partial shading of PV modules with
647 different connection configurations of PV cells, Energy, 36 (2011) 3069-3078.
648 [48] A.D. Dhass, E. Natarajan, L. Ponnusamy, Influence of shunt resistance on the
649 performance of solar photovoltaic cell, 2012 International Conference on Emerging
650 Trends in Electrical Engineering and Energy Management (ICETEEEM), 2012, pp. 382-
651 386.
652 [49] M.S. Benghanem, S.N. Alamri, Modeling of photovoltaic module and experimental
653 determination of serial resistance, J. Taibah Univ. Sci., 2 (2009) 94-105.
654 [50] G. Trentadue, D. Pavanello, E. Salis, M. Field, H. Müllejans, Determination of
655 internal series resistance of PV devices: repeatability and uncertainty, Meas. Sci.
656 Technol., 27 (2016) 055005.
657 [51] M.R. Islam, F. Rahman, W. Xu, Advances in Solar Photovoltaic Power Plants,
658 Springer Berlin Heidelberg2016.
659 [52] S. Chtita, C. Yassine, A. Derouich, J. Belkadid, Modeling and Simulation of a
660 Photovoltaic Panel Based on a Triple Junction Cells for a Nanosatellite, International
661 Symposium on Advanced Electrical and Communication Technologies (ISAECT), 2018.
662 [53] D. Pletcher, Z.Q. Tian, D. Williams, Developments in Electrochemistry: Science
663 Inspired by Martin Fleischmann, Wiley2014.
664 [54] A.J. Bard, L.R. Faulkner, Electrochemical methods: fundamentals and applications,
665 Wiley India Limited2004.

[55] C.G. Zoski, Handbook of Electrochemistry, Elsevier Science2007.

[56] E. Alvarez-Guerra, A. Dominguez-Ramos, A. Irabien, Design of the Photovoltaic Solar Electro-Oxidation (PSEO) process for wastewater treatment, Chem. Eng. Res. Des., 89 (2011) 2679-2685.

[57] S.N. Lvov, Introduction to Electrochemical Science and Engineering, Taylor & Francis2014.

[58] M. Panizza, G. Cerisola, Direct And Mediated Anodic Oxidation of Organic Pollutants, Chem. Rev., 109 (2009) 6541-6569.

[59] C.A. Martínez-Huitle, S. Ferro, Electrochemical oxidation of organic pollutants for the wastewater treatment: direct and indirect processes, Chem. Soc. Rev., 35 (2006) 1324-1340.

[60] J.-Y. Chen, C.-L. Hsieh, N.-Y. Hsu, Y.-S. Chou, Y.-S. Chen, Determining the Limiting Current Density of Vanadium Redox Flow Batteries, Energies, 7 (2014) 5863.

[61] S. König, M.R. Suriyah, T. Leibfried, Innovative model-based flow rate optimization for vanadium redox flow batteries, J. Power Sources, 333 (2016) 134-144.

[62] F. Pan, Q. Wang, Redox Species of Redox Flow Batteries: A Review, Molecules, 20 (2015) 20499-20517.

[63] P. Alotto, M. Guarnieri, F. Moro, Redox flow batteries for the storage of renewable energy: A review, Renew. Sust. Energ. Rev., 29 (2014) 325-335.

[64] R. Ye, D. Henkensmeier, S.J. Yoon, Z. Huang, D.K. Kim, Z. Chang, S. Kim, R. Chen, Redox Flow Batteries for Energy Storage: A Technology Review, J Electrochem. Energy, 15 (2018).

[65] W. Lu, X. Li, H. Zhang, The next generation vanadium flow batteries with high power density – a perspective, PCCP, 20 (2018) 23-35.

690 [66] M. Panizza, P.A. Michaud, G. Cerisola, C. Comninellis, Anodic oxidation of 2-
691 naphthol at boron-doped diamond electrodes, J. Electroanal. Chem., 507 (2001) 206-214.
692 [67] M. Panizza, P.A. Michaud, G. Cerisola, C. Comninellis, Electrochemical treatment
693 of wastewaters containing organic pollutants on boron-doped diamond electrodes:
694 Prediction of specific energy consumption and required electrode area, Electrochem.
695 Commun., 3 (2001) 336-339.
696 [68] A. Kapałka, G. Fóti, C. Comninellis, Investigations of electrochemical oxygen
697 transfer reaction on boron-doped diamond electrodes, Electrochim. Acta, 53 (2007) 1954-
698 1961.
699 [69] C.G. Piuleac, M.A. Rodrigo, P. Cañizares, S. Curteanu, C. Sáez, Ten steps modeling
700 of electrolysis processes by using neural networks, Environ. Modell. Softw., 25 (2010)
701 74-81.

702